이학석사 학위논문

Comparison of pelagic prokaryotic communities between two ice shelf regions of the Southern Ocean in late austral summer

늦여름 남빙양 두 빙붕 지역의 표영성 원핵생물 군집 비교

2023 년 8 월

서울대학교 대학원
지구환경과학부
신 동 영

Comparison of pelagic prokaryotic communities between two ice shelf regions of the Southern Ocean in late austral summer

늦여름 남빙양 두 빙붕 지역의

표영성 원핵생물 군집 비교

지도 교수 황 청 연

이 논문을 이학석사 학위논문으로 제출함

2023 년 5 월

서울대학교 대학원

지구환경과학부

신 동 영

신 동 영의 이학석사 학위논문을 인준함

2023 년 7 월

위 원 장 정 해 진 (인)

부위원장 황 청 연 (인)

위 원 김 종 성 (인)

Abstract

Comparison of pelagic prokaryotic communities between two ice shelf regions of the Southern Ocean in late austral summer

신동영 (Dong Young Shin)
지구환경과학부 (School of Earth and Environmental Sciences)
The Graduate School
Seoul National University

Ice shelf regions in the Southern Ocean are highly productive areas where dynamic water masses exist and large amounts of basal melt occur, but little is known about how environmental variables in the region influence marine prokaryotes and their activities. By sequencing the 16S rRNA gene, this study conducted a comparative analysis on pelagic prokaryotic community compositions of ice shelf regions, especially the Dotson Ice Shelf (DIS) region in the Amundsen Sea and the Nansen Ice Shelf (NIS) region in the Ross Sea. The results showed distinct patterns of prokaryotic community compositions in each region based on corresponding water masses. In the DIS region, *Flavobacteriia* were found to be prevalent in the epipelagic zone, whereas in the NIS region, *Alphaproteobacteria* emerged as the dominant taxa in the same zone. In both regions, the mesopelagic zone exhibited high species richness, with a wide range of taxa associated with important microbial processes in deep-sea environments. Notably, the prokaryotic communities in the DIS

region exhibited notable variations in relation to distances from the ice shelf. These variations strongly indicate the evident influences of meltwater, including the high relative abundance of *Nitrosopumilus spp.* in the meltwater-influenced area. Overall, the study provides insights into the differentiated compositions of epipelagic and mesopelagic prokaryotic communities in the DIS and NIS regions, highlighting the importance of meltwater influences on pelagic prokaryotic communities in ice shelf regions.

Keywords: Southern Ocean, Ice Shelf, Pelagic Prokaryotic Communities, Meltwater

Student Number: 2021-28355

Table of Contents

Abbreviations

AASW	Antarctic Surface Water
ANOSIM	Analysis of similarities
ASVs	Amplicon Sequence Variants
CDW	Circumpolar Deep Water
DIS	Dotson Ice Shelf
HSSW	High Salinity Shelf Water
NADW	North Atlantic Deep Water
NIS	Nansen Ice Shelf
nMDS	non-Metric Multidimensional Scaling
PCCs	Prokaryotic Community Compositions
PE	Paired-end
RDA	Redundancy analysis
RSSW	Ross Sea Surface Water
WW	Winter Water

List of Tables

List of Figures

1. Introduction

Despite facing harsh conditions such as low water temperatures and large environmental fluctuations, marine prokaryotic communities of the Southern Ocean play a crucial role in the global climate system. They affect global biogeochemical cycles through their carbon sequestration and transportation of nutrients to deep-sea environments [1, 2]. However, due to the rapid pace of global warming [3], the region experiences an annual loss of ice sheets and a change in water mass movements, which can significantly change its prokaryotic community compositions (PCCs) and prokaryotic activities [4-9].

Ice shelf regions are valuable spots for studying the impact of global warming on marine PCCs due to their significant amount of meltwater discharge from the shelves [10-12]. The Dotson Ice Shelf (DIS) in the Amundsen Sea of West Antarctica is known for its high basal melt rates by intrusion of Circumpolar Deep Water (CDW) [11]. Antarctic Surface Water (AASW) and Winter Water (WW) reside upon the CDW, forming distinct boundaries against each other [13]. Prokaryotic activities associated with light, iceberg movement, and phytoplankton bloom have been studied earlier in this region [6, 14, 15]. Meanwhile, the Nansen Ice Shelf (NIS) in the Ross Sea of East Antarctica shows much lower basal melt rates with low temperature and high salinity compared to the DIS [11]. It is because the intrusion of warm CDW is limited due to the Antarctic slope front formed by

salty deep water in the Ross Sea [16]. PCCs of the NIS region have been briefly studied for their relationships with water masses and sponges [17, 18].

Both the DIS and the NIS region are characterized by their active hydrological movements, driven by different water masses with unique environmental features [6, 18, 19]. These regions offer ideal locations to study the interactions between PCCs and water masses, as they exhibit varying degrees of basal melts and host different types of water masses in each respective region. However, the current microbiological data for these regions is incomplete, as it lacks information on archaeal data and data from the mesopelagic zone. Moreover, the high seasonal and annual variabilities of PCCs further complicate the comparison of previous data, making it challenging to draw comprehensive conclusions [20, 21]. Therefore, an intensive experimental design that encompasses a wide range of sampling areas, depths, and microbial taxa with consistent methodologies is required for a complete comparison of the PCCs in the ice shelf region.

In the summer of 2022, a study was conducted in the DIS and the NIS region to analyze the prokaryotic communities with sampling performed at depths spanning the entire water column. The objectives of this study were to compare the PCCs of each region using taxonomical and environmental data and to examine the meltwater influences that would possibly contribute to shaping the prokaryotic communities of the ice shelf regions.

2. Materials & Methods

2.1. Sampling

During the late austral summer of 2022 (January to March), a sampling expedition was conducted by the *R/V Araon* icebreaker of the Korea Polar Research Institute to gather data from two separate ice shelf regions in the Pacific Ocean Sector of the Southern Ocean. 25 stations near the DIS in the Amundsen Sea and 12 stations near the NIS in the Ross Sea were selected as the sampling sites (Figure 1). The Seabird 911 plus CTD sensor (Sea-Bird Scientific, USA) was utilized to monitor the environmental parameters such as water temperature, salinity, dissolved oxygen (DO), and fluorescence. The seawater samples were collected using 20 L Niskin bottles attached to the CTD, from the six chosen depths based on sensor profiles. Additionally, seawater samples were obtained from under the DIS through a borehole created by hot water drilling (station HWD, 74.3698° S, 112.5763° W).

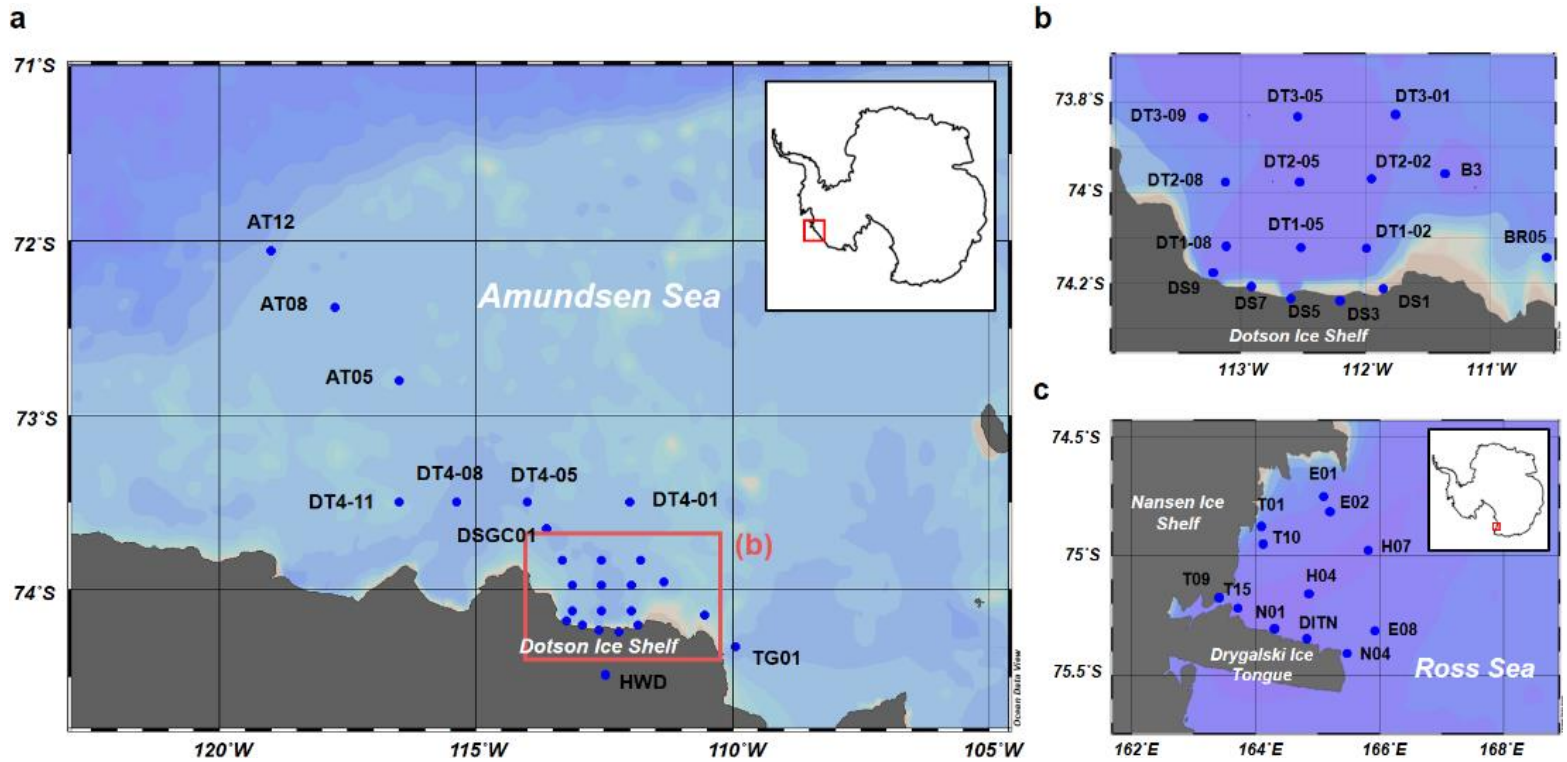

Figure 1 Location map of the study area and the sampling stations. **a** The location of the Amundsen Sea and its corresponding sampling stations, with the red box highlighting the stations located near the Dotson Ice Shelf (DIS) illustrated in Figure 1−b. **b** Detailed map of the stations near the DIS. **c** Map of the Ross Sea and Nansen Ice Shelf (NIS), with its sampling stations.

2.2. Prokaryotic Community Analysis

The seawater samples were filtered into particle-attached and free-living fractions using 3.0 μm and 0.2 μm membrane filters at each station depth. The filters were immediately stored at −80℃. Genomic DNA was extracted from the 0.2 μm membrane filters using the DNeasy Powersoil Pro Kit (MoBio Laboratories, USA), in accordance with the manufacturer's protocols. The V4-V5 region of the 16S rRNA gene was amplified using a set of barcoded 515F (5′ -GTGYCAGCMGCCGCGGTAA-3′) and 926R (CCGYCAATTYMTTTRAGTTT-3′) primers, following the methods from Jang *et al.* [22]. The barcoded PCR products were used for the construction of the library using the Nextra XT Index Kit (Illumina, USA) and were then sequenced by Illumina MiSeq PE (paired-end) system at LAS, South Korea.

Quality control and adaptor trimming were conducted using Trimmomatic version 0.29 [23]. The barcoded reads were demultiplexed with Cutadapt version 4.0 [24]. Additional quality control, paired-end merging, and read denoising were performed using DADA2 [25] in the Qiime2 environment [26]. Taxonomic assignments of all amplicon sequence variants (ASVs) were accomplished using the Greengenes database [27] and the RDP classifier [28]. Unassigned ASVs and non-prokaryotic taxa were excluded from further analyses.

2.3. Prokaryotic Abundance

The subsampled seawater samples were preserved with 0.02 μm filtered formalin (final concentration 2%) and stored at −20℃ for later analysis. In the laboratory, the fixed cells were thawed and stained with SYBR Green I (final concentration 1%) before being incubated at 35℃ for 30 minutes. The abundance of prokaryotic cells was determined using a BD Accuri C6 Plus flow cytometer (Becton Dickinson, USA) [29].

2.4. Nutrient Data

The subsamples for measuring the macronutrient concentrations were kept at −20℃ until analysis in the laboratory. The targeted macronutrients included ammonium (NH_4), nitrate (NO_3), nitrite (NO_2), phosphate (PO_4), and silicate (SiO_2). The concentrations of the nutrients were measured in triplicate using the QuAAtro AntoAnalyzer (SEAL Analytical, USA).

2.5. Statistical Analysis

Environmental variables, macronutrient concentrations, and prokaryotic abundance (PA) data were normalized using log transformation and Z-score normalization. The correlation matrix was visualized using the Corrgram package in R [30]. The Hellinger transformation was applied to the data matrix to solve double-zero asymmetry [31].

A curated ASV table generated from the taxonomic assignment was used for further statistical analyses. Rarefaction curves were plotted using the iNEXT package in R [32]. Alpha diversities (Shannon diversity and Chao1 richness) were calculated for each sample using Qiime2 software [26]. Spearman correlation coefficients between Shannon diversity and distances from the shelf were calculated, while the geographic distances were calculated using a spheroidal model of Earth [33], using PASSaGE version 2 [34].

To minimize the effect of sampling completeness, 2000 reads were rarefied for each sample before conducting the beta diversity analysis. Samples were grouped based on the water mass of origin, which was determined by the temperature, salinity, and DO signals obtained from CTD profiles. Bray-Curtis similarity matrices were then constructed to perform a non-metric multidimensional scaling (nMDS) analysis. This was done by using the metaMDS function in the Vegan package in R [35, 36]. To determine the degree of group separation by water mass, the Analysis of Similarities (ANOSIM)

was conducted using Qiime2 software based on 1000 permutations [26]. Redundancy analysis (RDA) was performed to further analyze the variations in PCCs under the influences of environmental factors, macronutrient concentrations, and prokaryotic abundances. The analysis was carried out using the Vegan package in R [35], and significant explanatory parameters ($p<0.05$) were obtained for the community structures. Distance-decay curves were drawn based on the Bray-Curtis similarity matrices and distances between the sampling stations. A Mantel test with 9999 permutations was used to assess the statistical association between the variables. For network analysis, the data was uploaded to the open-access network analysis pipeline (MENAP, http://ieg2.ou.edu/MENA) [37], following the general framework described in Zhang *et al.* [38].

3. Results

3.1. Overview of the Physicochemical and Biological Conditions

The temperature, salinity, dissolved oxygen (DO), and macronutrient profiles exhibited patterns consistent with known datasets (Figure 2 and 3). Specifically, the seawater in the DIS region displayed comparatively higher temperatures and lower salinity compare to the seawater in the NIS region. In both regions, the concentrations of NH_4, NO_2, and SiO_2 did not demonstrate significant variations with increasing depths. However, the concentrations of NO_3 and PO_4 increased as the depths increased.

Temperature, salinity, and DO data from the CTD have successfully differentiated the water masses in the DIS and the NIS region (Figure 4, 5, and Table 1). The distribution patterns of the water masses in both regions were found to be in accordance with past studies [13, 16]. The water masses present in the DIS consisted of AASW, WW, and CDW, with a total of 59, 23, and 31 samples classified into these water masses, respectively. Samples from the NIS region are assigned as Ross Sea Surface Water (RSSW) and High Salinity Shelf Water (HSSW), with 30 and 41 samples sorted into each category. The two ice shelf regions did not share common water masses, with the water masses in the NIS exhibiting relatively high salinity and low temperature.

FIECO-AFL fluorescence, which is an indirect measure of

chlorophyll concentrations of the seawater, showed a significant difference in 5 m depth between the DIS and the NIS region (Figure 6). The relative fluorescence was rated high in the DIS region, while the fluorescence was rated relatively low around all the sampling sites in the NIS region.

The summary of PAs is presented in Figure 7. PAs were in the order of 10^5 ml^{-1}, a typical range in the near-ice shelf regions of the Southern Ocean [6, 14]. The PAs of each region decreased with increasing depth. The average PA values were higher the in the NIS than in the DIS.

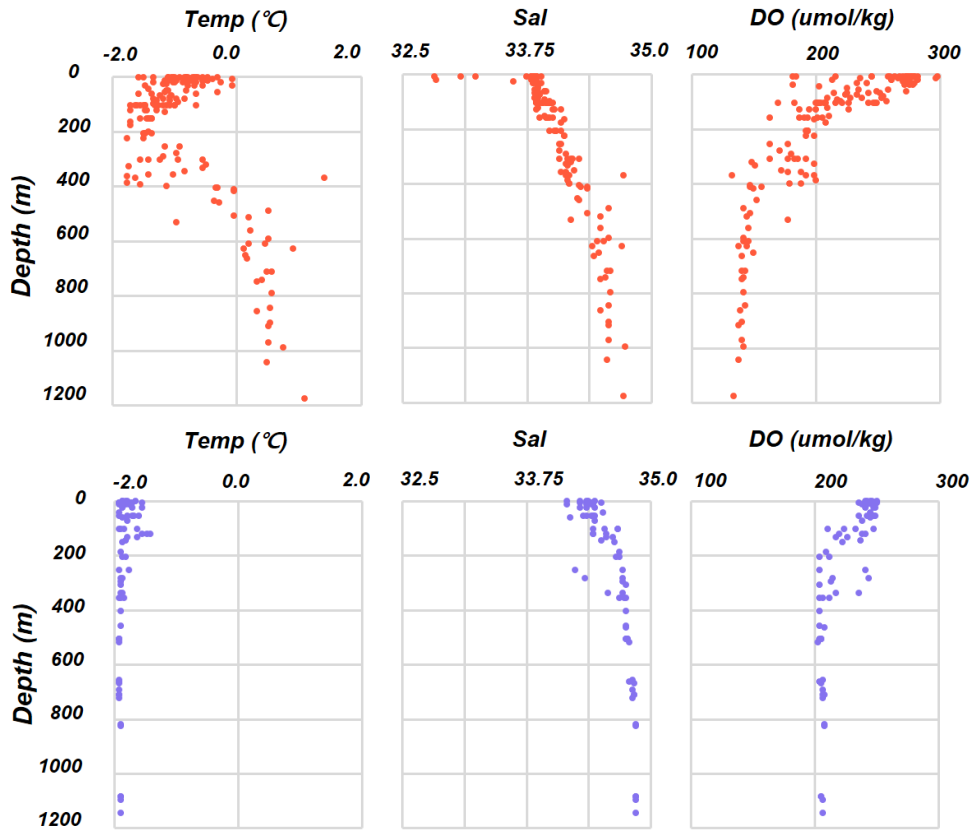

Figure 2 Temperature, salinity, and dissolved oxygen (DO) profiles from each ice shelf region. The upper graphs indicate the values in the Dotson Ice Shelf region, indicated with red dots, and the lower graphs indicate the values in the Nansen Ice Shelf region, indicated with purple dots.

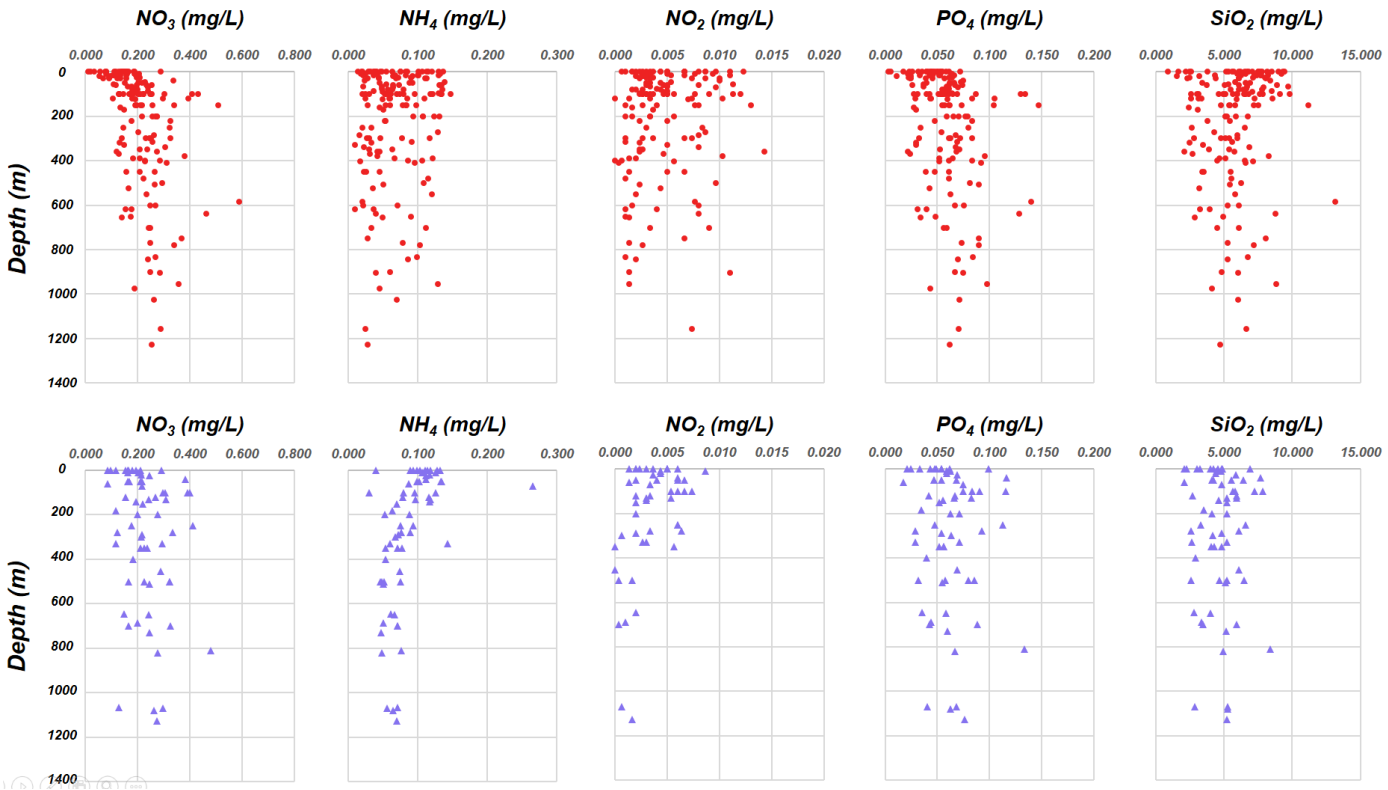

Figure 3 Macronutrient profiles from each ice shelf region. The upper graphs indicate the macronutrient concentration by depth in the Dotson Ice Shelf region, indicated with red dots, and the lower graphs indicate the macronutrient concentration by depth in the Nansen Ice Shelf region, indicated with purple triangles.

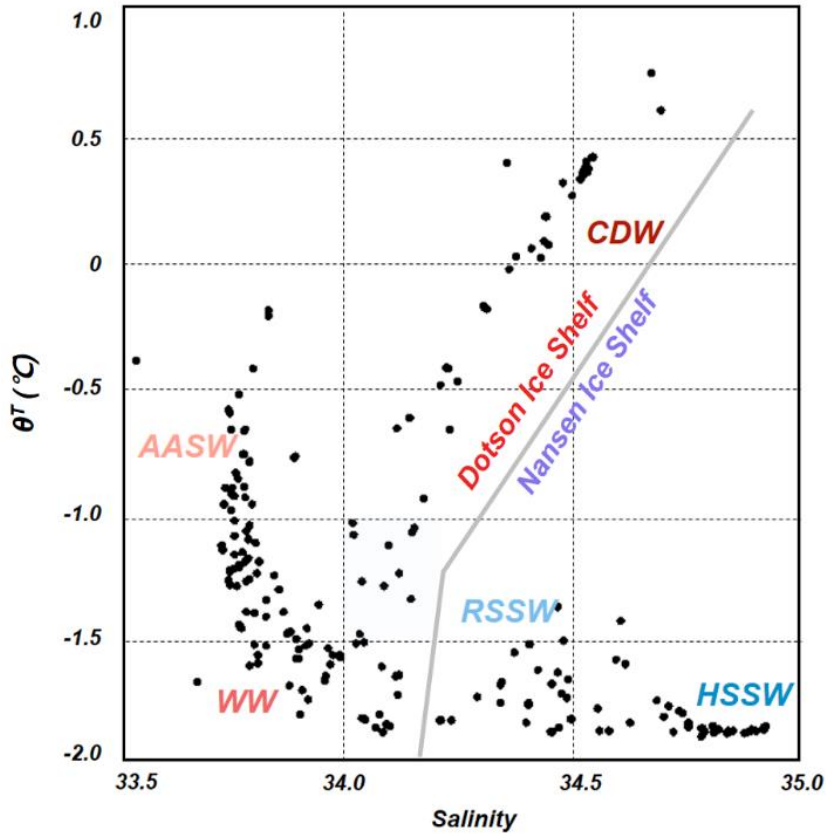

Figure 4 TS diagram presenting all data from this study.

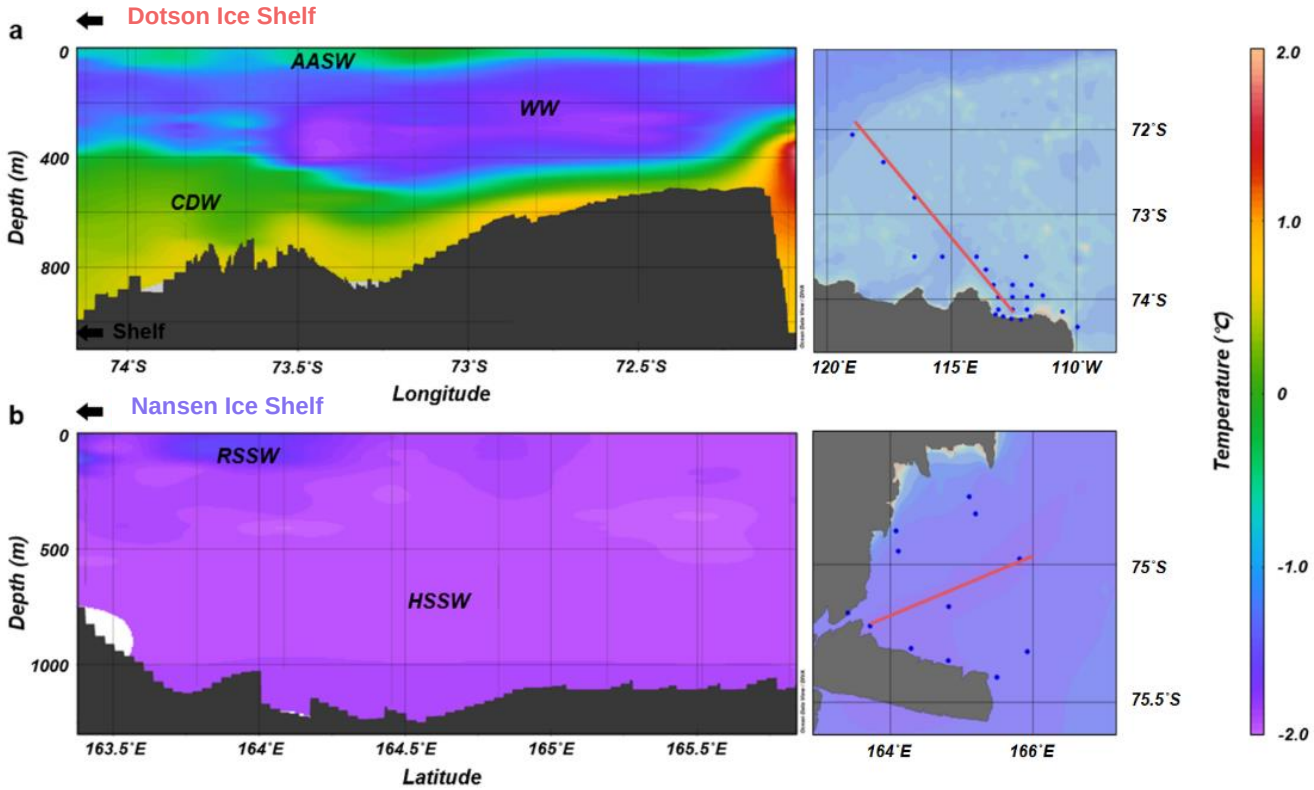

Figure 5 a Temperature distribution in the Dotson Ice Shelf region of the Amundsen Sea, with the corresponding water masses indicated. The location of the depicted area is shown on the map on the right. **b** Temperature distribution in the Nansen Ice Shelf region of the Ross Sea, with the corresponding water mass names indicated. The location of the depicted area is shown on the map on the right.

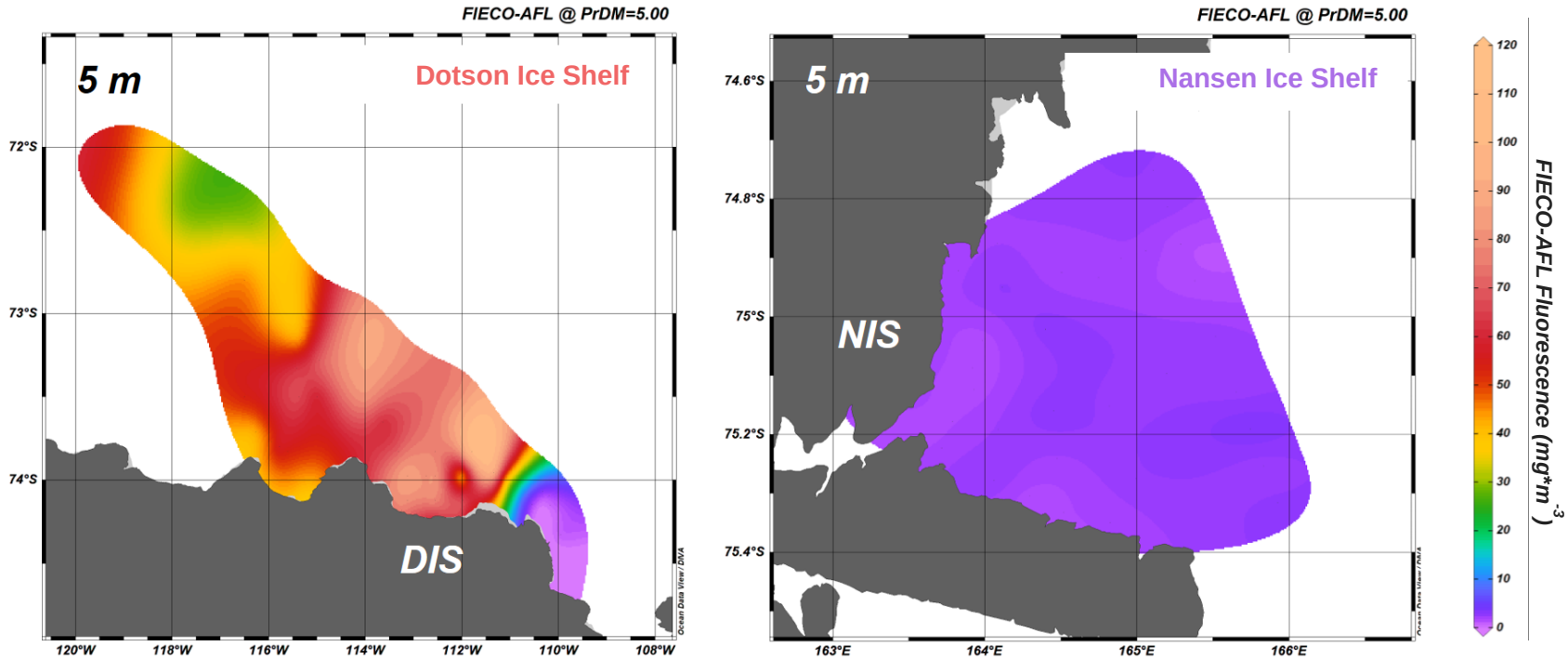

Figure 6 FIECO-AFL fluorescence measured from the CTD casting in each region, from 5 m depths.

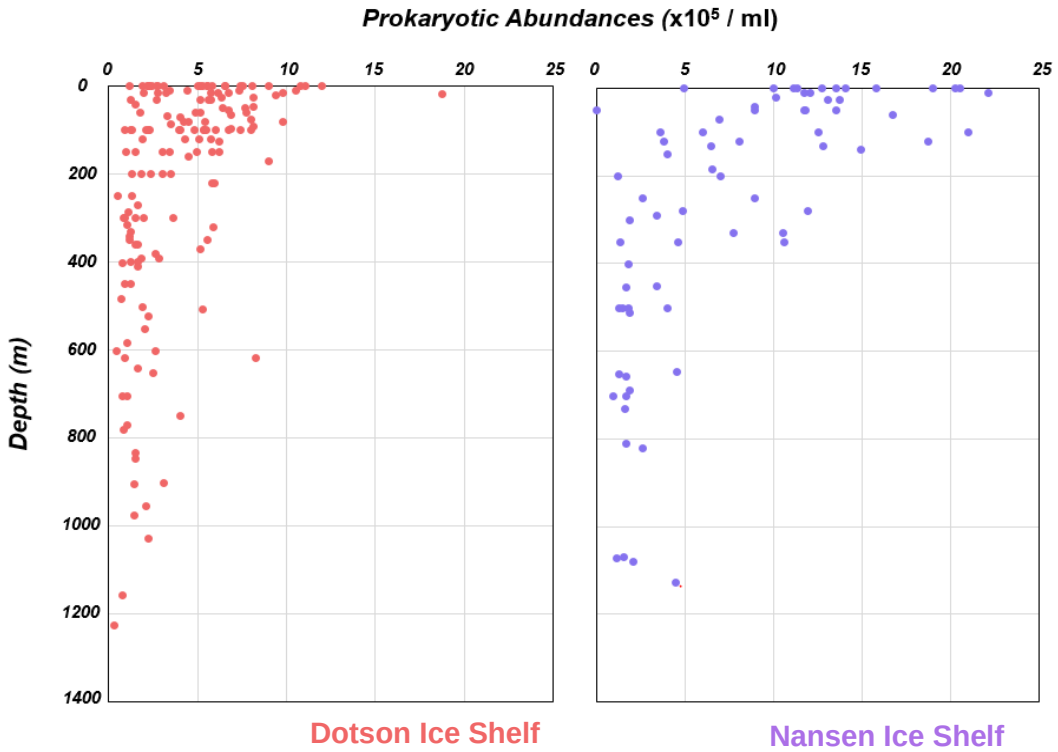

Figure 7 Estimated prokaryotic abundances by depth for each ice shelf region. Samples from the Dotson Ice Shelf region are indicated with red dots, and the samples from the Nansen Ice Shelf region are indicated with purple dots.

Table 1 Summary of sample counts per water masses with their approximate ranges of depth, temperature, salinity, and dissolved oxygen concentrations.

Sea		**Amundsen Sea**		**Ross Sea**	
Ice Shelf Region		**Dotson Ice Shelf**		**Nansen Ice Shelf**	
Water Mass	**AASW**	**WW**	**CDW**	**RSSW**	**HSSW**
Depth (m)	0 − 100	100 − 400	> 400	0 − 200	> 200
Temperature (℃)	-1.5 − 0.0	-2.0 − -1.5	-1.5 − -1.0	-1.0 − -2.0	< -1.5
Salinity	33.5 − 34.0	33.5 − 34.2	34.0 − 35.0	34.0 − 34.7	> 34.7
DO (umol/kg)	300 − 400	250 − 350	150 − 250	300 − 350	250 − 300
Sample Count	59	23	31	30	41

3.2. Vertical Variations in the Prokaryotic Communities

The sequencing of the V4−V5 region in the 16S rRNA gene from 225 samples generated a total of 3,888,790 reads. Following the steps of trimming, denoising, chimera removal, and taxa filtration, 2,002,931 high−quality reads and 2,292 ASVs were retained. Individual samples yielded 437 to 31,718 (mean 8,823) reads in total. The rarefaction curves for observed ASVs reached saturation (Figure 8), indicating that a sufficient level of sampling has been conducted for all stations and depths.

Calculated alpha diversity indexes (Shannon diversity and Chao1 richness) are depicted in Figure 9 and listed in Table 2. Both the Shannon diversity and Chao1 richness indexes increased with depth in each region. The Chao1 richness of surface waters from the two regions was comparable, while the Shannon diversity was higher in the RSSW compared to the AASW. The differences in the indexes were higher in the DIS region.

To analyze and visualize the patterns of PCCs in the DIS and NIS region, the constructed ASV table was subjected to nMDS analysis (Figure 10). With a stress value of 0.12 in nMDS, the PCCs of each sampling region were distinguished into five distinct clusters, based on their corresponding regions and water masses. To confirm the accuracy of sample separation based on water mass properties, an ANOSIM was performed. The results of the analysis showed a high R statistic of 0.881 ($p<0.001$), indicating that samples were

effectively assigned to specific groups based on water mass properties. The R statistics for ANOSIM within individual DIS and NIS, based on water mass properties, were 0.856 and 0.507 ($p<0.001$), respectively.

RDA was used to examine how variations in PCCs are influenced by environmental variables (Figure 11). Depth, temperature, salinity, PA, DO, and macronutrient concentrations were included as candidates in a stepwise forward selection procedure. In the DIS region of the Amundsen Sea, the variables that had the strongest effect on the PCCs were DO, salinity, temperature, and NH_4, in order of strength. These variables explained approximately 51% of the PCCs. The statistically significant explanatory variable in the NIS region of the Ross Sea was DO, which explained approximately 35% of the PCCs.

The taxonomically assigned reads of the samples based on water mass properties are summarized in Table 3 and depicted in Figure 12 and Figure 13. In the DIS region in the Amundsen Sea, the PCCs were dominated by *Flavobacteriia* and *Proteobacteria*, accounting for more than 50% of the total PCCs. However, the relative proportions of the two phyla varied between water masses. In the AASW, characterized by high prokaryotic abundances and low alpha diversity, *Flavobacteriia*, *Alphaproteobacteria*, *Gammaproteobacteria*, and *Crenarchaeota* were the dominant taxa accounting for more than 90% of the total PCCs. In the WW, the proportion of *Flavobacteriia* decreased from a mean of 46.27% to 20.81% in the total PCCs, while the proportions of *Crenarchaeota* and *Deltaproteobacteria* increased

from 5.81% to 11.79% and 2.34% to 6.26%, respectively. The CDW showed relatively even PCCs, with *Flavobacteriia* (16.60%), *Crenarchaeota* (22.33%), *Deltaproteobacteria* (10.92%), *Euryarchaeota* (5.56%), and *Verrucomicrobia* (3.03%) making up large proportions of the communities.

In the NIS region of the Ross Sea, the patterns of PCCs in the RSSW and the HSSW were distinct from those in the DIS region of the Amundsen Sea. The PCC in the RSSW was dominated by *Flavobacteriia* and *Proteobacteria*, which account for about 90% of the water mass. In RSSW, *Alphaproteobacteria* was the most prevalent class in the environment, making up an average of 40.49% of the PCCs. *Flavobacteriia* and *Gammaproteobacteria* were less dominant, constituting 33.67% and 12.59% of the PCCs, respectively. In the HSSW, the proportion of *Flavobacteriia* and *Alphaproteobacteria* decreased to 23.14% and 27.27% respectively, while the proportion of *Crenarcheaota*, *Deltaproteobacteria*, *Euryarchaeota*, and *Verrucomicrobia* increased to 10.73%, 8.97%, 3.44%, and 2.52% respectively. Notably, the proportion of *Planctomycetes* rose abnormally high compared to other water masses in this study, reaching 4.57%. The proportion of *Gammaproteobacteria* remained consistent in both water masses of the NIS region.

Based on the correlations between taxa abundance in the prokaryotic communities, network analysis was conducted. Within each water mass, network topological indexes including average connectivity (avgK) and modularity were calculated (Figure 14).

AvgK measures the complexity of a network, with higher values indicating a more complex network [37]. Network modularity can be thought of as microbial functional units or niches, with modularity being the extent to which a network can be partitioned into modules or communities [37]. The complexity of the network varied with depth in the two ice shelf regions. In both regions, network complexity increased with depth. The highest avgK value was observed in the RSSW with a score of 24.145. Modularity was the highest in the CDW, scoring 0.512.

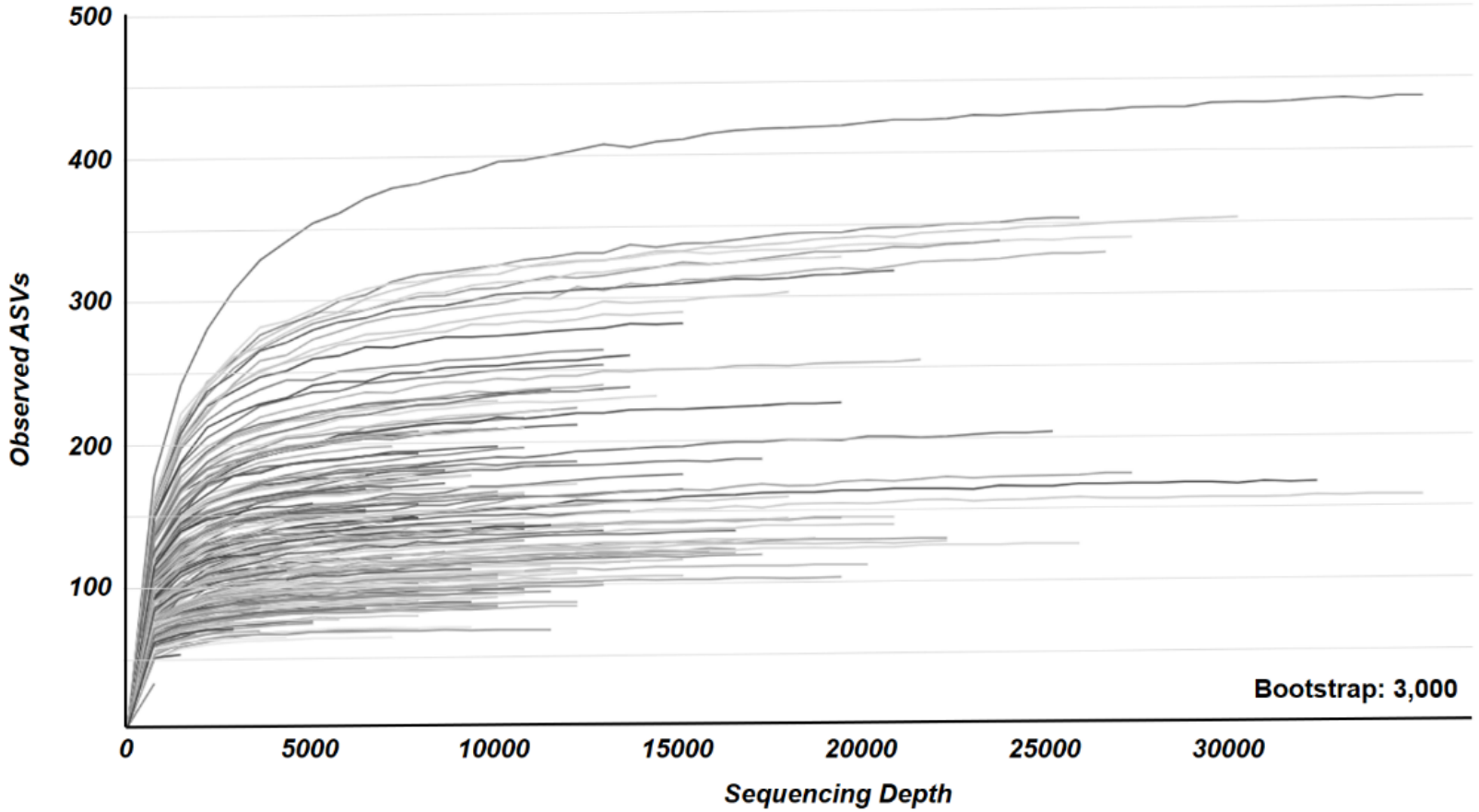

Figure 8 The rarefaction curves for observed Amplicon Sequence Variants (ASVs) per sequencing depth (read counts per samples). The bootstrap value used in the analysis was set at 3000.

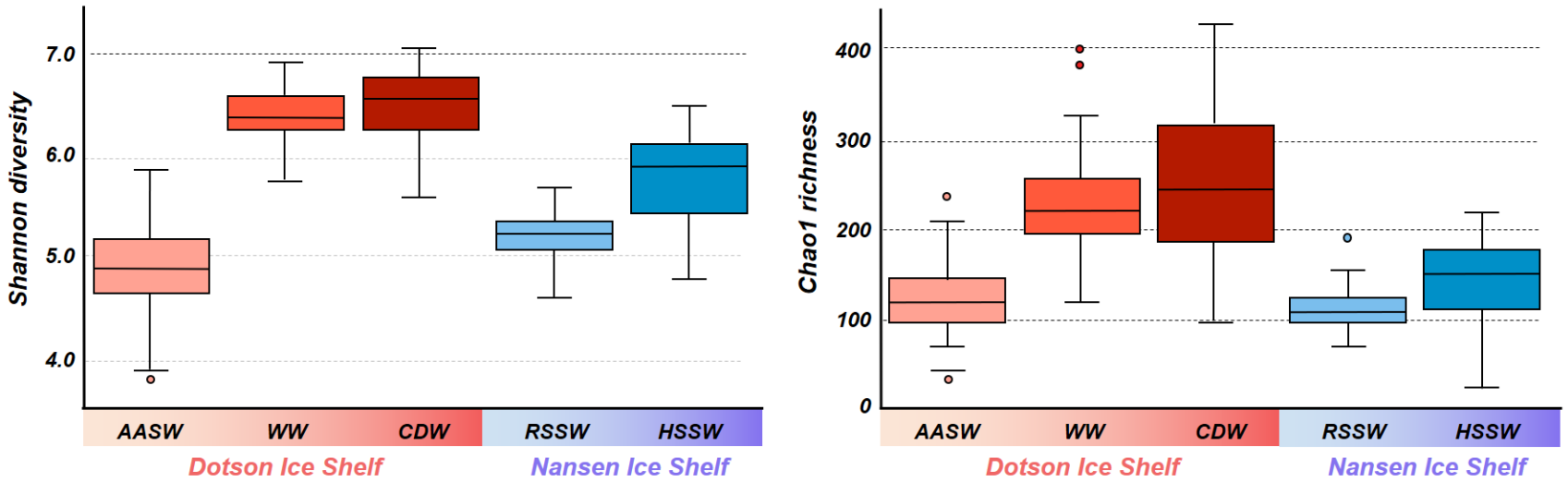

Figure 9 Boxplots of alpha diversity indexes based on water mass properties. Shannon diversity (left) and Chao1 richness (right).

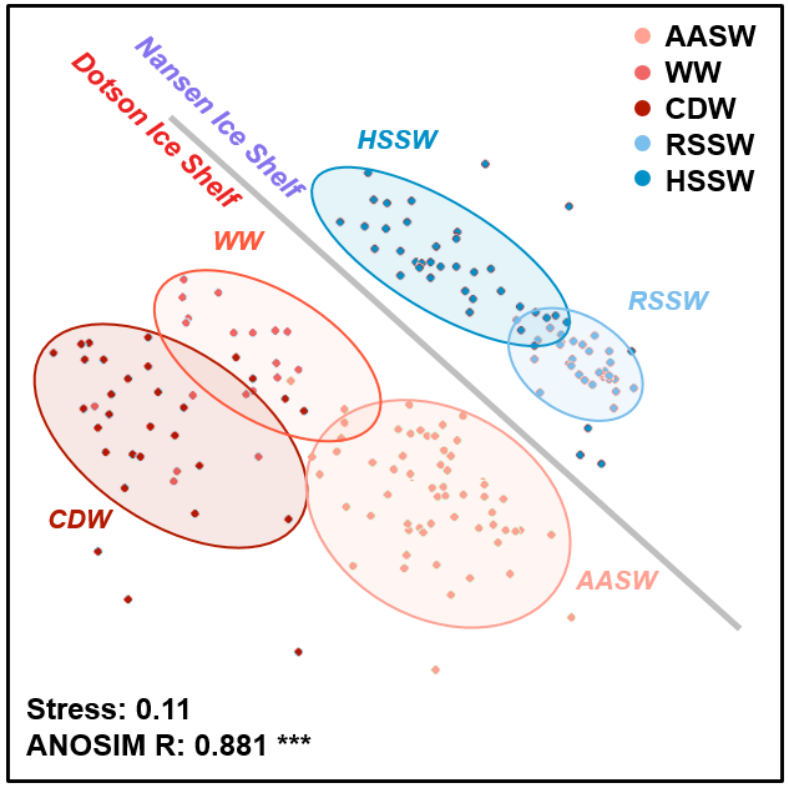

Figure 10 The results of non-Metric Multidimensional Scaling (nMDS) analysis based on Bray-Curtis dissimilarities of the prokaryotic community compositions (PCCs), with a stress value of 0.11. Each point is colored based on the water mass properties.

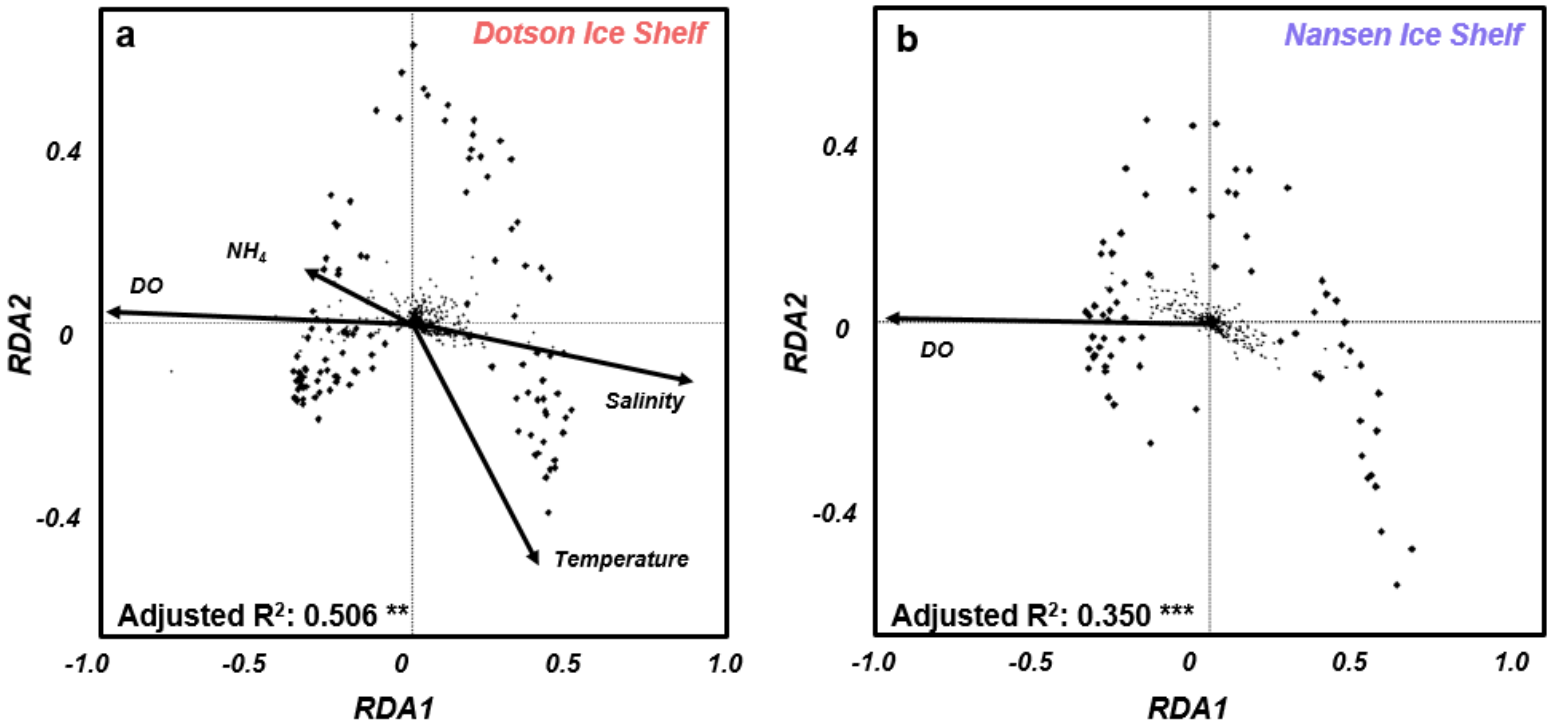

Figure 11 Results from redundancy analysis (RDA) in the Dotson Ice Shelf (DIS) region of the Amundsen Sea(a) and in the Nansen Ice Shelf (NIS) region of the Ross Sea(b) in scaling 2. Each dot in the graph represents an individual sample. Longer arrows indicate variables that strongly influence the variation in the communities, and the direction of each arrow represents correlations between the two arrows.

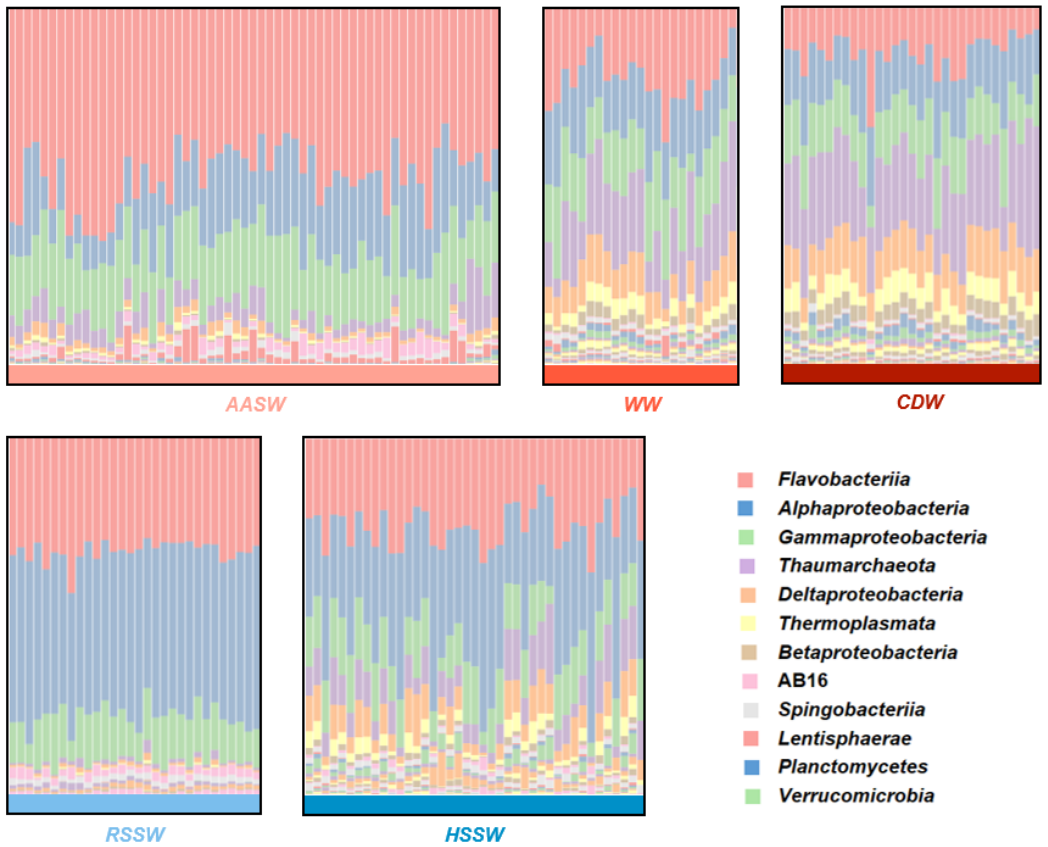

Figure 12 The relative abundance of prokaryotic phyla in each water mass. The colors on the labels correspond to their respective regions. The detailed data for the PCCs can be found in **Table 3**.

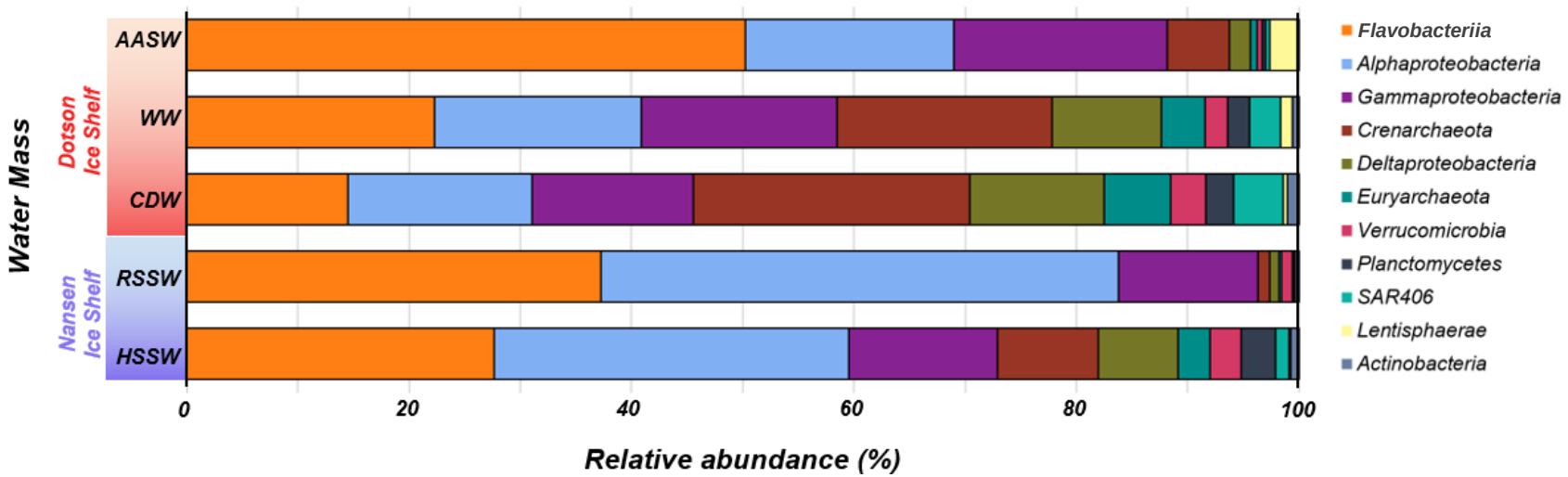

Figure 13 The taxonomic bar plots divided by their corresponding water masses. Each result of taxonomic assignments is color coded.

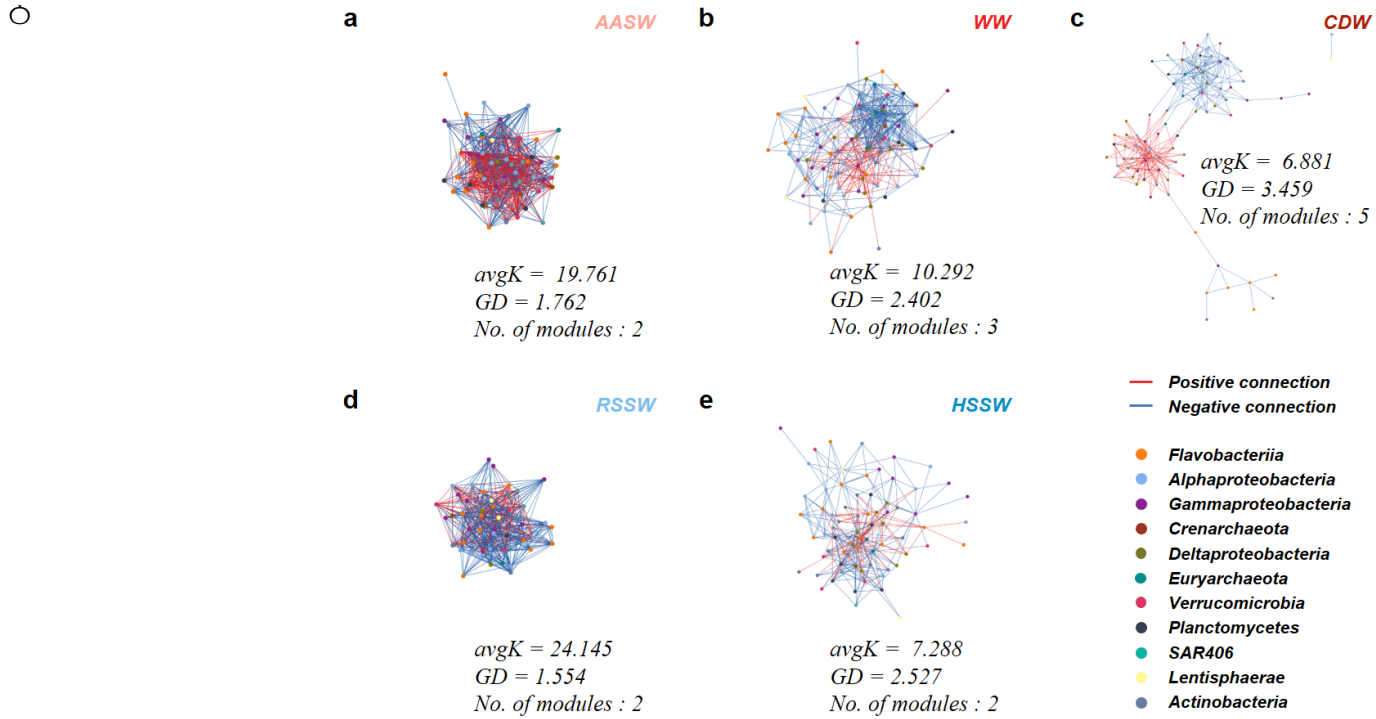

Figure 14 Network interactions between OTUs in each water mass. Each line connects two OTUs, with red lines indicating positive interactions suggesting mutualism or cooperation, and blue lines indicating negative interactions suggesting predation or competition. The nodes are color-coded according to their phyla on the lower right of the figure. The network topological indexes, including *avgK* (average connectivity) and modularity, are displayed.

Table 2 Summary of sample counts per water masses with their prokaryotic abundances, Shannon diversity, and Chao1 richness.

Sea	Ice Shelf Region	Water mass	Ranging Depths (m)	Sample count (#)	Prokaryotic abundance ($\times 10^5$ ml^{-1})	Shannon diversity	Chao1 richness
					Mean (±s.d.)	Mean (±s.d.)	Mean (±s.d.)
Amundsen Sea	Dotson Ice Shelf	AASW	0 – 100	59	5.6 (±2.1)	4.9 (±0.4)	128 (±38)
		WW	100 – 400	23	1.8 (±1.0)	6.4 (±0.3)	238 (±69)
		CDW	> 400	31	1.5 (±0.8)	6.5 (±0.4)	256 (±97)
Ross Sea	Nansen Ice Shelf	RSSW	0 – 200	30	13.4 (±4.3)	5.2 (±0.2)	114 (±24)
		HSSW	> 200	41	4.0 (±3.2)	5.7 (±0.5)	142 (±44)

Table 3 Relative abundances of prokaryotes at the class level, sorted by sampling regions and water mass properties.

Region	Relative abundances (%)				
	Amundsen Sea			Ross Sea	
WaterMass	AASW	WW	CDW	RSSW	HSSW
	Mean (±s.d.)	Mean (±s.d.)	Mean (±s.d.)	Mean (±s.d.)	Mean (±s.d.)
Flavobacteriia	46.27 (±11.86)	32.00 (±9.53)	16.60 (±11.91)	33.67 (±6.04)	23.14 (±5.61)
Alphaproteobacteria	20.81 (±7.86)	21.46 (±0.32)	15.89 (±3.25)	40.49 (±8.41)	27.27 (±6.55)
Gammaproteobacteria	18.82 (±4.50)	17.22 (±0.82)	14.42 (±3.59)	12.59 (±3.42)	13.25 (±4.80)
Crenarchaeota	5.81 (±5.74)	11.79 (±6.57)	22.33 (±7.96)	3.78 (±4.09)	10.73 (±4.53)
Deltaproteobacteria	2.34 (±2.57)	6.26 (±0.84)	10.92 (±3.08)	2.85 (±3.42)	8.97 (±3.63)
Euryarchaeota	0.76 (±1.02)	2.39 (±2.09)	5.56 (±1.92)	1.17 (±1.67)	3.44 (±1.56)
Verrucomicrobia	0.61 (±0.71)	1.47 (±1.15)	3.03 (±0.98)	1.79 (±1.58)	2.52 (±1.66)
Planctomycetes	0.32 (±0.41)	1.25 (±1.14)	2.25 (±1.02)	0.83 (±1.44)	4.57 (±2.43)
SAR406	0.50 (±0.79)	1.57 (±1.28)	3.94 (±1.38)	0.50 (±0.70)	1.38 (±0.54)
Betaproteobacteria	1.24 (±0.63)	1.50 (±0.91)	1.05 (±0.39)	1.63 (±0.32)	1.57 (±0.56)
Others	2.51 (±0.17)	3.09 (±0.25)	4.00 (±0.15)	0.72 (±0.04)	3.16 (±0.10)

3.3. Horizontal Variations in the Prokaryotic Communities

A significant correlation was observed by calculating the Shannon diversity index in relation to geographical distances from the shelf ($p<0.01$) (Figure 15). The index showed an increase with distance in the AASW, while it exhibited a decrease with distance in the WW and the CDW. The calculated Spearman correlation coefficients were 0.375, −0.605, and −0.365 in the AASW, WW, and CDW, respectively.

The Bray−Curtis similarity matrix was used to measure the similarity between pairs of prokaryotic communities. Then the similarity is calculated as a function of the geographic distances between each pair of sampling sites (Figure 16), with the significance tested with the Mantel test. In the DIS region, prokaryotic communities of each water mass displayed a consistent decrease in community similarities with increasing geographic distances. The gradients of decaying curves were steeper in the AASW (−0.12, $p<0.001$) and the WW (−0.14, $p<0.001$) compared to the gradient in the CDW (−0.06, $p<0.001$). Conversely, prokaryotic communities in the HSSW did not show decaying patterns while PCCs from the RSSW showed consistently high similarities between the samples regardless of their proximities, with a little gradient of decaying patterns (−0.06, $p<0.001$).

Salinity distributions around the DIS region were depicted in Figure 17, illustrating the potential meltwater−influenced area. From 10 m depth to 400 m depth, salinity was low around the shelf and

increased as it went further from the shelf. The samples assigned to the WW were further divided into two categories, namely meltwater-influenced WW and non-influenced WW, based on the salinity profiles obtained from the CTD data. In the studied taxa, *Nitrosopumilus spp.* exhibited significant variations in its relative abundance. Specifically, it was found to be 20.01% in the meltwater-influenced WW and 13.85% in the non-influenced WW(Figure 18).

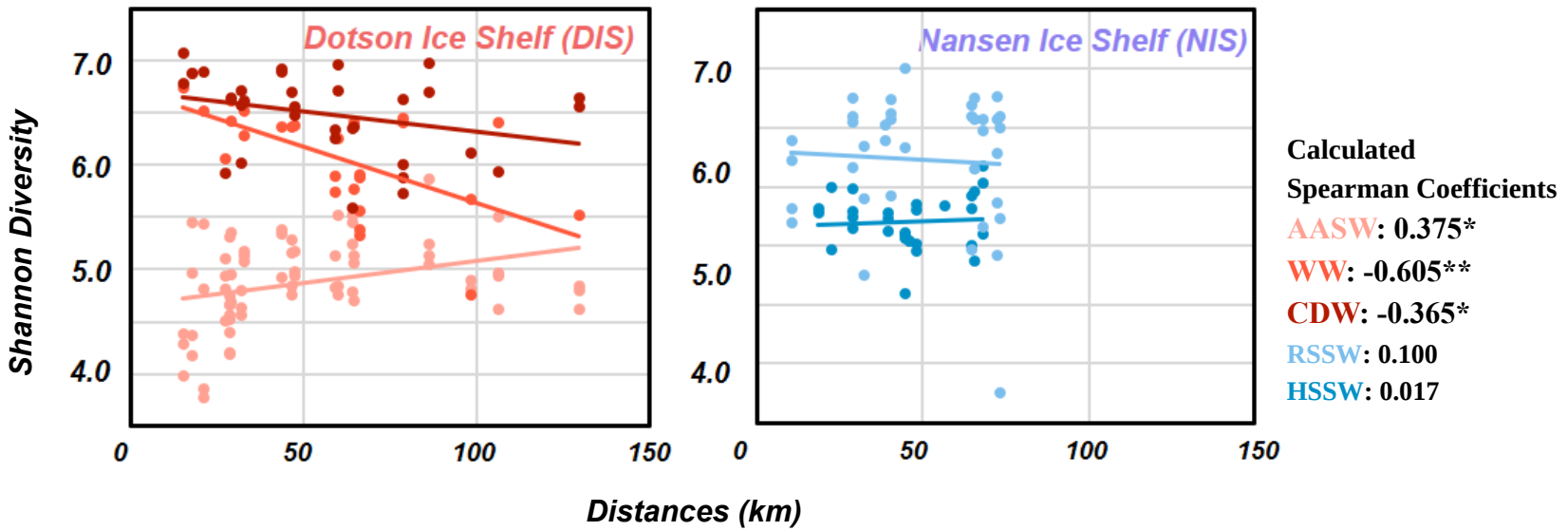

Figure 15 Shannon diversity index as a function of distances from the ice shelf. Spearman correlation coefficients were calculated, with their significance indicated with asterisks (*p<0.05, **p<0.01)

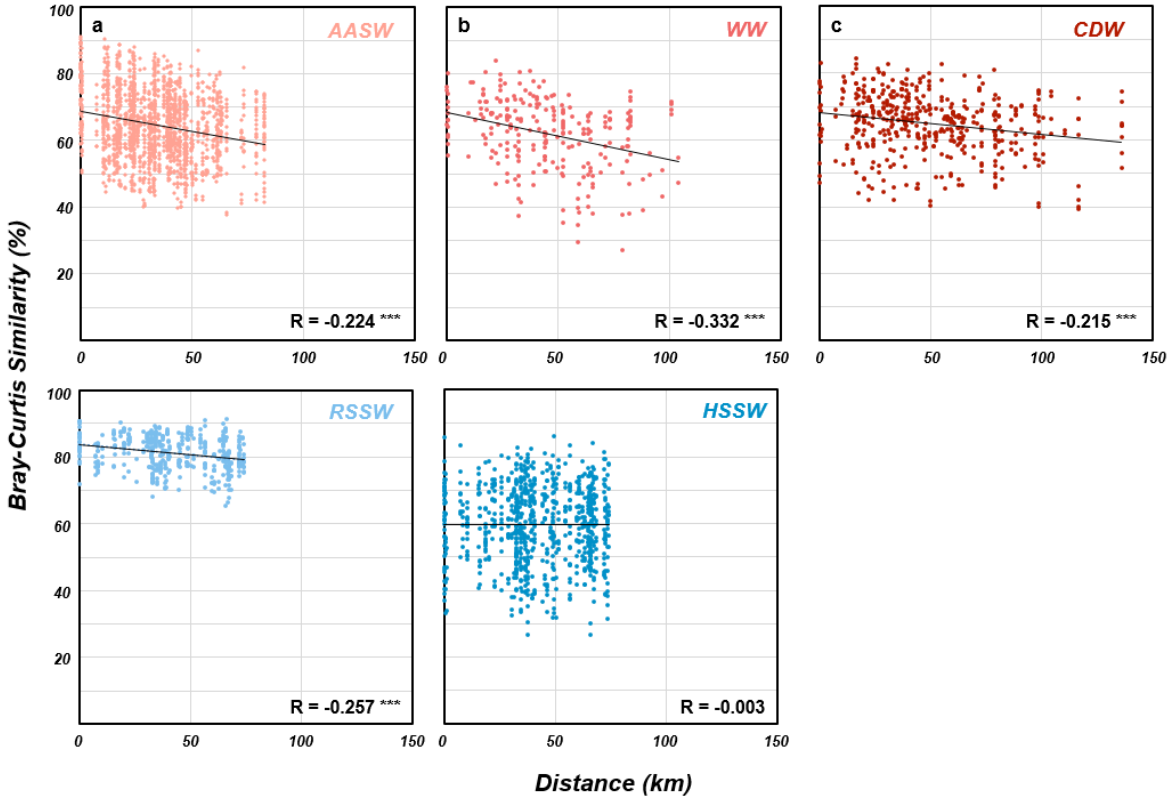

Figure 16 Distance-decay curves from all water masses, displaying the Bray-Curtis similarities between pairs of communities as a function of geographic distances between each sampling site. The black solid lines show the overall direction of the data. R statistics from the Mantel test are indicated on the bottom right side of each graph (***p<0.001).

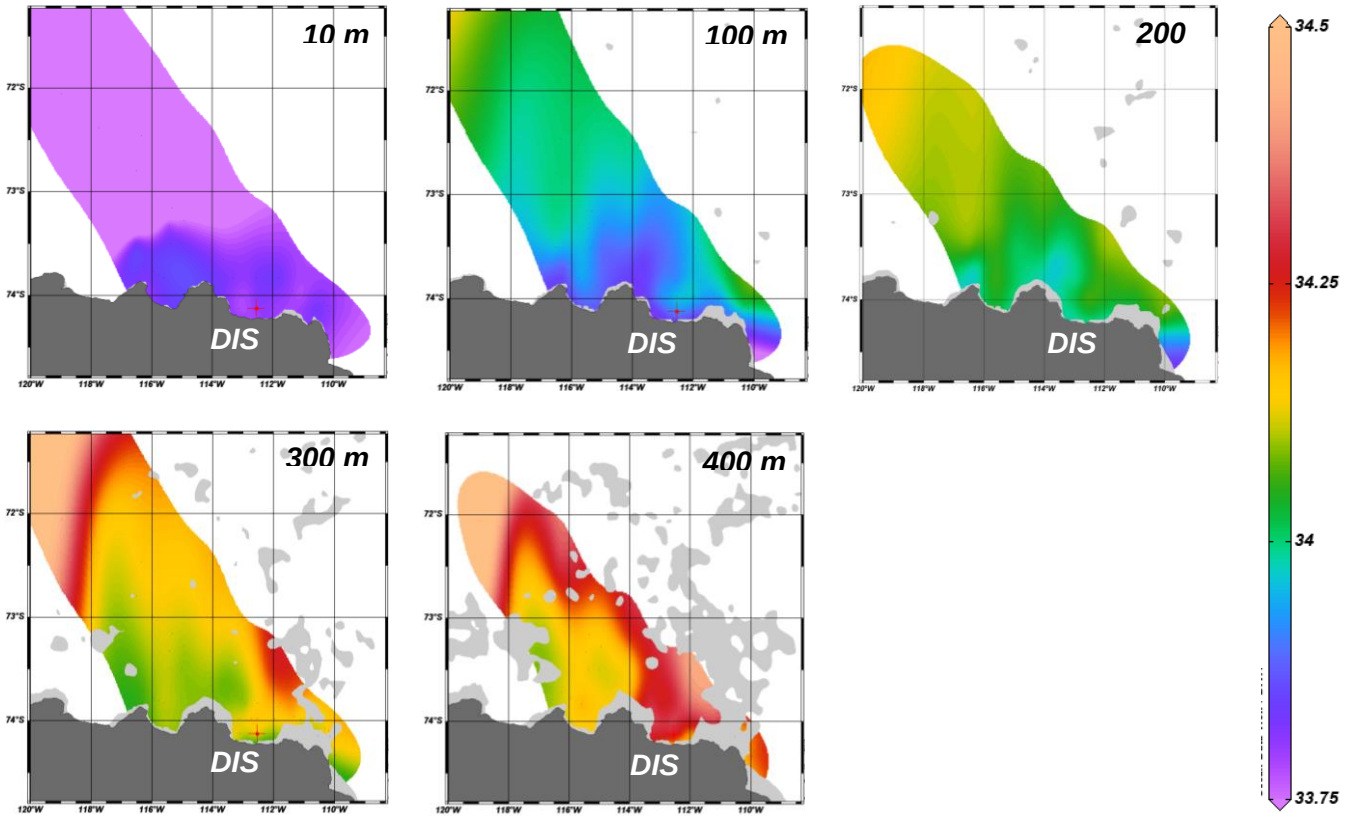

Figure 17 Salinity distributions in the Dotson Ice Shelf (DIS) region, from 10 m, 100 m, 200 m, 300 m, and 400 m depths.

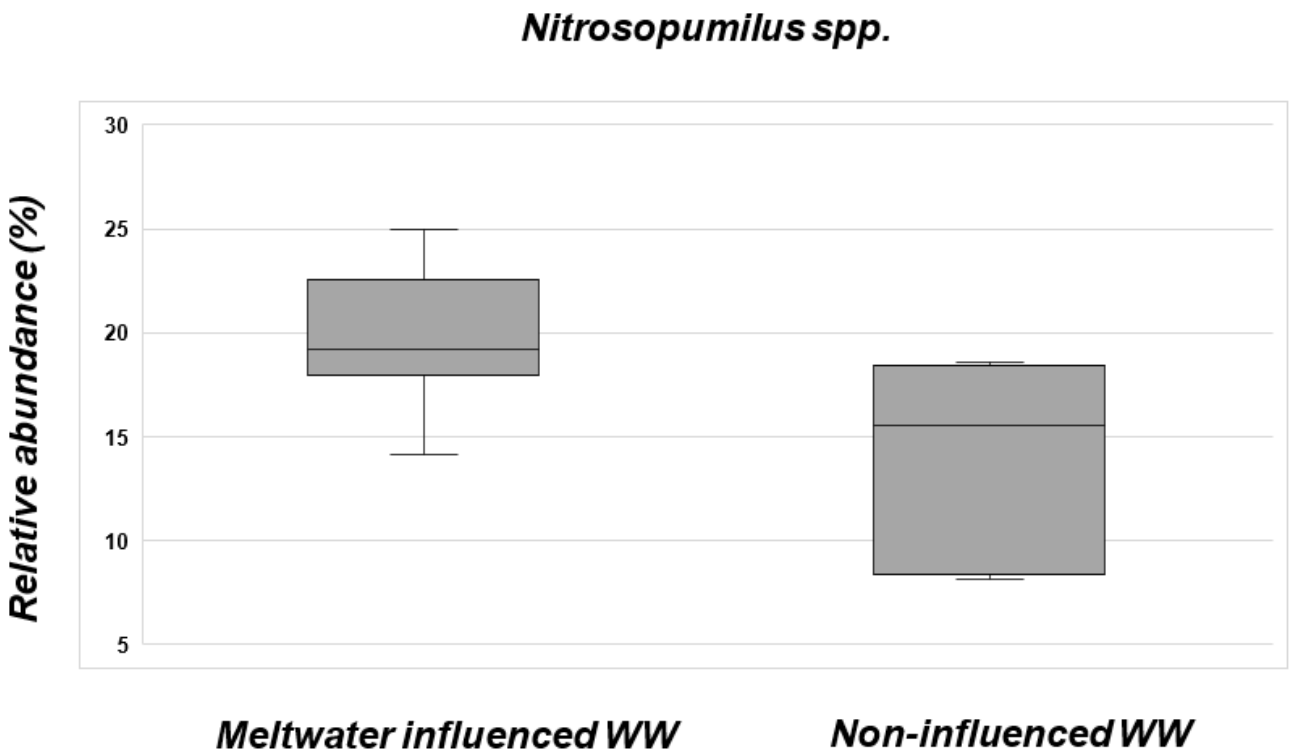

Figure 18 Relative abundances of *Nitrosopumilus spp.* from low salinity winter water (WW) and high salinity winter water.

Discussion

4.1. Differentiated Compositions of the Epipelagic Communities from the Two Ice Shelf Regions

The phytoplankton growth in the coastal Southern Ocean is recognized for its ability to homogenize prokaryotic communities, leading to relatively low community evenness within the surface water [39]. The haptophyte *Phaeocystis Antarctica*, which is known for dominating during the austral summer near the DIS [40], may have played a crucial role in lowering species richness within the AASW of the DIS region (Figure 7, 9, and Table 2). The low concentrations of NO_3 and PO_4 from the surface layer in the DIS region (Figure 3) and the relatively high fluorescence signal detected from the DIS region (Figure 6) suggest a considerable amount of phytoplankton growth taking place in the area [41, 42].

The taxonomic analysis provided additional confirmation (Figure 12, 13, and Table 3), revealing that a significant proportion of the PCCs consisted of copiotrophs that adapted to phytoplankton growth, including *Flavobacteriia*, *Gammaproteobacteria*, SAR92, and *Oceanospirillaceae* [14, 40, 43]. *Flavobacteriia*, which exhibited the highest relative abundance in the AASW, encompass bacteria that are commonly found in marine and freshwater environments [44]. These bacteria have been specifically associated with the uptake and breakdown of polymeric dissolved organic matter [44]. Some members of *Flavobacteriia* exhibit maximal growth rates during *P.*

Antarctica blooms that are nearly 2-fold higher than those of other abundant bacterial groups [45], supporting their high relative abundances in the AASW.

In contrast to the epipelagic zone of the DIS region, the dominant presence of *Alphaproteobacteria* rather than *Flavobacteriia* in the surface water of the NIS region is largely attributed to the SAR11 clade. This clade is well-known for its preference for low molecular weight dissolved organic matter in the Southern Ocean [5, 46]. The relatively low rates of phytoplankton growth implied by the low fluorescence signal detected from the NIS region (Figure 6) may have favored the SAR11 clade, which exhibits high adaptability to cold waters with limited concentrations of organic carbon [39, 46].

The free-living prokaryotes investigated from both regions may have derived benefits from the degradation of smaller molecules that had been diffused away from particles generated in the surface layer. The prokaryotes from the epipelagic zone that closely cooperate and compete with each other to utilize the molecules may have promoted metabolic collaboration, ultimately resulting in a high level of network complexity at the epipelagic zone (Figure 14).

4.2. High Prokaryotic Diversities in the Mesopelagic Zone

Heterotrophs thrive while diverse niches are created by the input of fresh and labile organic matter that sinks beneath the euphotic zone [47]. In the DIS region, a significant proportion of the particulate organic carbon derived from the *P. Antarctica* growth is recycled through bacterial respiration within the upper 400 meters of the water column, which is an approximate lower boundary of the WW [48, 49]. Therefore, an increase in organic and inorganic nutrients from the sinking particles may have contributed to the high species richness observed in the WW located under the AASW (Figure 9) [39].

Conversely, at depths below 400 meters, the cascading effect diminishes due to a decline in particle flux through remineralization [39]. Therefore, the distinct origin of the CDW from the North Atlantic Deep Water (NADW) is hypothesized to play a role in the high species richness observed in the deep CDW (Figure 9) [50]. The dynamic surface conditions lead to rapid speciation, whereas the deep water originated from NADW experiences relatively constant environmental conditions over longer periods of time. This longer timescale provides sufficient opportunity for the selection of phenotypes that are well-adapted to those specific conditions, resulting in high phylogenetic diversities [21, 50].

Similar patterns of prokaryotic distributions have been examined from the mesopelagic zone of the NIS region. The increase in alpha diversity (Shannon diversity and Chao1 richness) and decrease in PA

by depth were observed (Figure 7, 9, and Table 2).

The taxonomic analysis further supported the high species richness in deep water masses, demonstrating the enrichment of specific taxa involved in crucial microbial processes to deep-sea environments (Figure 12, 13, and Table 3). In both ice shelf regions, there was an evident increase in the relative abundance of SAR324 and SAR406 clades, known for their involvement in carbon fixation, sulfur cycling, and nitrous oxide reduction [4]. Additionally, *Planctomycetes*, which constitute a significant heterotrophic bacterial group that utilizes recalcitrant organic materials [51], were found in relatively high abundances in deep-sea environments. A previous study revealed that a substantial portion of the benthic microbial community in the DIS region (averaging 40% of the sequenced community) was affiliated with the phylum *Planctomycetes* [52], suggesting the connection between deep-sea communities and benthic communities.

4.3. Potential Meltwater Influences in the DIS Region

While the comparison of two separate ice shelf regions with different basal melt rates, several pieces of evidence implied meltwater influences on the marine PCCs of the DIS region. In the DIS region, a significant increase or decrease in Shannon diversity was observed with distance in all three water masses, which was not observed in the NIS region (Figure 15). The distance–decay curves also demonstrated that the Bray–Curtis similarities from the AASW and the WW exhibited a sharp decline with increasing distance from the shelf (Figure 16). Considering the eastward inflow and westward outflow containing meltwater at depths above 400 meters in the DIS region [53], the influence of meltwater would directly impact the WW, which is located in the upper 400 m depth range. No consistent changing patterns in PCCs were observed in the NIS region, which further suggests the limited influence of meltwater in the NIS region [11, 12].

In order to thoroughly examine the impact of meltwater on prokaryotic communities in the DIS region, salinity signals above a depth of 400 m were analyzed to identify regions potentially influenced by meltwater in the WW. The results revealed a significantly high relative abundance (mean of 20.01%) of *Nitrosopumilus spp.* in the meltwater–influenced WW. *Nitrosopumilus spp.* is recognized as an ammonia oxidizing archaea and has been reported to thrive in the presence of high ammonium concentrations originating from meltwater sources [54]. It is

interesting to note that in the RDA result, among the environmental variables examined in the DIS region, the concentration of ammonium stands out as the only explanatory variable alongside temperature, DO, and salinity (Figure 11). Another study has highlighted the iron requirements of *Nitrosopumilus*, suggesting that its growth may be limited by the availability of iron [55]. The substantial relative abundance observed in this study supports the notion that *Nitrosopumilus* can serve as a biomarker indicating meltwater influences in the Southern Ocean.

Conclusion

The Southern Ocean holds significant importance in the global carbon cycle and the regulation of Earth's climate. It accounts for approximately 40% of the total uptake of anthropogenic CO_2 by the ocean [56]. It is characterized by high biological productivity, especially in areas such as the continental shelf and coastal ice shelf zones [57, 58].

This study presents compelling evidence that the vertical structure of pelagic prokaryotic communities in two distinct ice shelf regions is strongly influenced by the properties of the underlying water masses. Notably, there is a clear segregation of communities between surface and mesopelagic waters, with different dominant taxa observed in each region. As we move deeper into the water column, diversities and network correlations exhibit significant variations, indicating substantial shifts in community composition and interactions. Furthermore, the study highlights the significant impact of contrasting melt rates on the organization and distribution of prokaryotic communities within the ice shelf regions, with notable differences observed depending on the distances from the DIS, including the high relative abundance of *Nitrosopumilus spp.* in the meltwater-influenced WW.

It is worth noting that this is the first direct comparison of two separate ice shelves using intensive-scale sampling and multi-depth analysis employing high-throughput sequencing techniques. Further

research is necessary to gain a better understanding of the potential drivers behind these patterns, and it is recommended to conduct multiple analyses, including measurements of iron concentrations, to elucidate additional factors at play. Additionally, an approach that incorporates simultaneous modeling of water mass movements would be valuable, as advection has been recognized as a significant factor shaping microbial assemblages in the Southern Ocean [5].

References

1 Cavicchioli, R., Microbial ecology of Antarctic aquatic systems. Nat Rev Microbiol, 2015. 13(11): p. 691-706.

2 Rath, J., et al., High phylogenetic diversity in a marine-snow-associated bacterial assemblage. Aquatic Microbial Ecology, 1998. 14(3): p. 261-269.

3 Schmidtko, S., et al., Multidecadal warming of Antarctic waters. Science, 2014. 346(6214): p. 1227-31.

4 Wilkins, D., et al., Key microbial drivers in Antarctic aquatic environments. FEMS Microbiol Rev, 2013. 37(3): p. 303-35.

5 Wilkins, D., et al., Advection shapes Southern Ocean microbial assemblages independent of distance and environment effects. Nat Commun, 2013. 4: p. 2457.

6 Dinasquet, J., et al., Mixing of water masses caused by a drifting iceberg affects bacterial activity, community composition and substrate utilization capability in the Southern Ocean. Environ Microbiol, 2017. 19(6): p. 2453-2467.

7 Hernando-Morales, V., J. Ameneiro, and E. Teira, Water mass mixing shapes bacterial biogeography in a highly hydrodynamic region of the Southern Ocean. Environ Microbiol, 2017. 19(3): p. 1017-1029.

8 Hamdan, L.J., et al., Ocean currents shape the microbiome of Arctic marine sediments. Isme Journal, 2013. 7(4): p. 685-696.

9 Alonso-Saez, L., et al., High archaeal diversity in Antarctic

circumpolar deep waters. Environmental Microbiology Reports, 2011. 3(6): p. 689-697.

10 Adusumilli, S., et al., Interannual variations in meltwater input to the Southern Ocean from Antarctic ice shelves. Nat Geosci, 2020. 13(9): p. 616-620.

11 Rignot, E., et al., Ice-shelf melting around Antarctica. Science, 2013. 341(6143): p. 266-70.

12 Silvano, A., S.R. Rintoul, and L. Herraiz-Borreguero, Ocean-Ice Shelf Interaction in East Antarctica. Oceanography, 2016. 29(4): p. 130-143.

13 Randall-Goodwin, E., et al., Freshwater distributions and water mass structure in the Amundsen Sea Polynya region, Antarctica. Elementa-Science of the Anthropocene, 2015. 3.

14 Richert, I., et al., The influence of light and water mass on bacterial population dynamics in the Amundsen Sea Polynya. Elementa-Science of the Anthropocene, 2015. 3.

15 Lee, Y., et al., Phytoplankton growth rates in the Amundsen Sea (Antarctica) during summer: The role of light. Environ Res, 2022. 207: p. 112165.

16 Friedrichs, D.M., et al., Observations of submesoscale eddy-driven heat transport at an ice shelf calving front. Communications Earth & Environment, 2022. 3(1).

17 Papale, M., et al., Exploring the Diversity and Metabolic Profiles of Bacterial Communities Associated With Antarctic Sponges (Terra Nova Bay, Ross Sea). Frontiers in Ecology and Evolution, 2020. 8.

18 Celussi, M., et al., Water masses' bacterial community structure and microbial activities in the Ross Sea, Antarctica. Antarctic Science, 2010. 22(4): p. 361-370.

19 Pardo, P.C., et al., Water masses distribution in the Southern Ocean: Improvement of an extended OMP (eOMP) analysis. Progress in Oceanography, 2012. 103: p. 92-105.

20 Luria, C.M., et al., Seasonal Succession of Free-Living Bacterial Communities in Coastal Waters of the Western Antarctic Peninsula. Front Microbiol, 2016. 7: p. 1731.

21 Ghiglione, J.F. and A.E. Murray, Pronounced summer to winter differences and higher wintertime richness in coastal Antarctic marine bacterioplankton. Environ Microbiol, 2012. 14(3): p. 617-29.

22 Jang, J., et al., Abundance and diversity of antibiotic resistance genes and bacterial communities in the western Pacific and Southern Oceans. Sci Total Environ, 2022. 822: p. 153360.

23 Bolger, A.M., M. Lohse, and B. Usadel, Trimmomatic: a flexible trimmer for Illumina sequence data. Bioinformatics, 2014. 30(15): p. 2114-2120.

24 Martin, M., Cutadapt removes adapter sequences from high-throughput sequencing reads. EMBnet. journal, 2011. 17(1): p. 10-12.

25 Callahan, B.J., et al., DADA2: High-resolution sample inference from Illumina amplicon data. Nat Methods, 2016. 13(7): p. 581-3.

26 Bolyen, E., et al., Reproducible, interactive, scalable and

extensible microbiome data science using QIIME 2 (vol 37, pg 852, 2019). Nature Biotechnology, 2019. 37(9): p. 1091-1091.

27 McDonald, D., et al., An improved Greengenes taxonomy with explicit ranks for ecological and evolutionary analyses of bacteria and archaea. ISME J, 2012. 6(3): p. 610-8.

28 Wang, Q., et al., Naive Bayesian classifier for rapid assignment of rRNA sequences into the new bacterial taxonomy. Appl Environ Microbiol, 2007. 73(16): p. 5261-7.

29 Gasol, J.M. and P.A. Del Giorgio, Using flow cytometry for counting natural planktonic bacteria and understanding the structure of planktonic bacterial communities. Scientia Marina, 2000. 64(2): p. 197-224.

30 Friendly, M., Corrgrams: Exploratory displays for correlation matrices. American Statistician, 2002. 56(4): p. 316-324.

31 Legendre, P. and D. Borcard, Box-Cox-chord transformations for community composition data prior to beta diversity analysis. Ecography, 2018. 41(11): p. 1820-1824.

32 Hsieh, T.C., K.H. Ma, and A. Chao, iNEXT: an R package for rarefaction and extrapolation of species diversity (Hill numbers). Methods in Ecology and Evolution, 2016. 7(12): p. 1451-1456.

33 Winter, C., B. Matthews, and C.A. Suttle, Effects of environmental variation and spatial distance on bacteria, archaea and viruses in sub-polar and arctic waters. ISME J, 2013. 7(8): p. 1507-18.

34 Rosenberg, M.S. and C.D. Anderson, PASSaGE: pattern analysis, spatial statistics and geographic exegesis. Version 2. Methods in Ecology and Evolution, 2011. 2(3): p. 229-232.

35 Dixon, P., VEGAN, a package of R functions for community ecology. Journal of Vegetation Science, 2003. 14(6): p. 927-930.

36 Clarke, K.R., et al., Change in marine communities: an approach to statistical analysis and interpretation. 2014.

37 Zhou, J., et al., Functional molecular ecological networks. mBio, 2010. 1(4).

38 Zhang, Y., W. Xiao, and N. Jiao, Linking biochemical properties of particles to particle-attached and free-living bacterial community structure along the particle density gradient from freshwater to open ocean. Journal of Geophysical Research: Biogeosciences, 2016. 121(8): p. 2261-2274.

39 Richert, I., et al., Summer comes to the Southern Ocean: how phytoplankton shape bacterioplankton communities far into the deep dark sea. Ecosphere, 2019. 10(3).

40 Delmont, T.O., et al., Phaeocystis antarctica blooms strongly influence bacterial community structures in the Amundsen Sea polynya. Frontiers in Microbiology, 2014. 5.

41 Paytan, A. and K. McLaughlin, The oceanic phosphorus cycle. Chemical Reviews, 2007. 107(2): p. 563-576.

42 Pollard, R., P. Treguer, and J. Read, Quantifying nutrient supply to the Southern Ocean. Journal of Geophysical Research-Oceans, 2006. 111(C5).

43 Kim, J.G., et al., Unveiling abundance and distribution of planktonic Bacteria and Archaea in a polynya in Amundsen Sea, Antarctica. Environmental Microbiology, 2014. 16(6): p. 1566-1578.

44 Kirchman, D.L., New light on an important microbe in the ocean. Proceedings of the National Academy of Sciences of the United States of America, 2008. 105(25): p. 8487-8488.

45 Zeder, M., et al., A small population of planktonic Flavobacteria with disproportionally high growth during the spring phytoplankton bloom in a prealpine lake. Environmental Microbiology, 2009. 11(10): p. 2676-2686.

46 Dinasquet, J., M. Landa, and I.I. Obernosterer, SAR11 clade microdiversity and activity during the early spring blooms off Kerguelen Island, Southern Ocean. Environmental Microbiology Reports, 2022. 14(6): p. 907-916.

47 Jiao, N., et al., Microbial production of recalcitrant dissolved organic matter: long-term carbon storage in the global ocean. Nature Reviews Microbiology, 2010. 8(8): p. 593-599.

48 Ducklow, H.W., et al., Particle flux on the continental shelf in the Amundsen Sea Polynya and Western Antarctic Peninsula. Elementa-Science of the Anthropocene, 2015. 3.

49 Lee, S., et al., Evidence of minimal carbon sequestration in the productive Amundsen Sea polynya. Geophysical Research Letters, 2017. 44(15): p. 7892-7899.

50 Sow, S.L.S., et al., Biogeography of Southern Ocean prokaryotes: a comparison of the Indian and Pacific sectors. Environmental Microbiology, 2022. 24(5): p. 2449-2466.

51 Wilkins, D., et al., Key microbial drivers in Antarctic aquatic environments. FEMS Microbiology Reviews, 2013. 37(3): p. 303-335.

52 Cho, H., et al., A Unique Benthic Microbial Community Underlying the Phaeocystis antarctica-Dominated Amundsen Sea Polynya, Antarctica: A Proxy for Assessing the Impact of Global Changes. Frontiers in Marine Science, 2020. 6.

53 Yang, H.W., et al., Seasonal variability of ocean circulation near the Dotson Ice Shelf, Antarctica. Nature Communications, 2022. 13(1).

54 Zhu, Y.Y., E.B. Searle, and H.Y.H. Chen, Functionally and phylogenetically diverse boreal forests promote sapling recruitment. Forest Ecology and Management, 2022. 524.

55 Shafiee, R.T., et al., Iron requirements and uptake strategies of the globally abundant marine ammonia-oxidising archaeon, Nitrosopumilus maritimus SCM1. Isme Journal, 2019. 13(9): p. 2295-2305.

56 Gruber, N., et al., Oceanic sources, sinks, and transport of atmospheric CO2. Global Biogeochemical Cycles, 2009. 23.

57 Montes-Hugo, M.A. and X.J. Yuan, Climate patterns and phytoplankton dynamics in Antarctic latent heat polynyas. Journal of Geophysical Research-Oceans, 2012. 117.

58 Arrigo, K.R., G.L. van Dijken, and A.L. Strong, Environmental controls of marine productivity hot spots around Antarctica. Journal of Geophysical Research-Oceans, 2015. 120(8): p. 5545-5565.

초록

남빙양의 빙붕 지역은 역동적인 수괴 움직임과 대량의 기저 용융이 나타나는 고생산성 지역으로, 이 지역의 환경 변수가 해양의 원핵생물과 그들의 활동에 어떤 영향을 미치는지에 대해서는 아직 알려지지 않은 바가 많다. 본 연구는 16S rRNA 유전자 시퀀싱을 통해 남극의 빙붕 지역, 그 중에서도 아문젠해의 닷슨 빙붕 지역(Dotson Ice Shelf, DIS)과 로스해의 난센 빙붕 지역(Nansen Ice Shelf, NIS)의 표영성 원핵생물 군집 조성에 대한 비교 분석을 수행하였다. 그 결과 각 지역과 수괴에 대응하는 독특한 표영성 원핵생물 군집 조성의 패턴이 나타났다. 닷슨 빙붕 지역에서는 *Flavobacteriia*가 상대적으로 풍부하게 나타났으며, 난센 빙붕 지역에서는 *Alphaproteobacteria*가 동일한 깊이에서 우세한 생물종으로 나타났다. 양 지역의 중층대에서는 심해 환경에서 중요한 미생물 프로세스와 관련된 다양한 분류군이 나타나는 것을 확인하였다. 특히 닷슨 빙붕 지역의 원핵생물 군집은 빙붕으로부터의 거리에 따라 뚜렷한 변동성을 나타내었다. 이러한 변동은 빙붕 용융을 포함한 용융수의 뚜렷한 영향을 강력하게 시사하고 있으며, 용융수의 영향을 받는 지역에서 *Nitrosopumilus spp.*의 상대적인 풍부도가 높은 것이 확인되었다. 이 연구는 닷슨 빙붕 지역 및 난센 빙붕 지역의 표층대와 중층대 군집의 차이를 명확하게 보여주며, 빙붕 지역의 표영성 원핵생물 군집에의 용융수 영향의 중요성을 보여준다.

주요어: 남빙양, 표영성 원핵생물 군집, 용융수
학번: 2021-28355